Measuring Smoothness of Real-Valued Functions Defined by Sample Points on the Unit Circle

Stephan Weiss[1], Ian K. Proudler[1], and Malcolm D. Macleod[1,2]
[1]Dept. Electronic & Electrical Engineering, University of Strathclyde, Glasgow G1 XW, Scotland
[2] QinetiQ Ltd., Malvern, Hertfordshire, UK
{stephan.weiss,ian.proudler,malcolm.macleod}@strath.ac.uk

***Abstract*—In the context of extracting analytic eigen- or singular values from a polynomial matrix, a suitable cost function is the smoothness of continuous, real, and potentially symmetric periodic functions. This smoothness can be measured as the power of the derivatives of that function, and can be tied to a set of sample points on the unit circle that may be incomplete. We have previously explored the utility of this cost function, and here provide refinements by (i) analysing properties of the cost function and (ii) imposing additional constraints on its evaluation.**

I. Introduction

For a matrix $\boldsymbol{R}(z) : \mathbb{C} \rightarrow \mathbb{C}^{M\times M}$ that comprises rational analytic functions in the variable $z \in \mathbb{C}$ and is parahermitian such that $\boldsymbol{R}^{\mathrm{P}}(z) = \boldsymbol{R}^{\mathrm{H}}(1/z^*) = \boldsymbol{R}(z)$ [1], a parahermitian matrix eigenvalue decomposition (EVD) with analytic factors exists in almost all cases [2], [3]. These may generally be transcendental functions and as such absolutely convergent Laurent series. If the decomposition is approximated by Laurent polynomials, the choice for the factors widens, and include others, such as spectrally majorised solutions, which time domain polynomial matrix EVD algorithms [4]–[8] encourage or even guarantee [9] to obtain. The difference between these solutions is contrasted in Fig. 1. In comparison, discrete Fourier transform (DFT) domain algorithms [10]–[13] can permit a choice to extract approximations of both spectrally majorised and analytic solutions.

DFT-domain algorithms do not naturally possess the frequency domain coherence that has motivated time domain approaches [4], [5], [7], and therefore require association across frequency bins. In [10]–[12] this association is based on the continuity of eigenvectors, which in principle is easier to detect than a non-differentiability of eigenvalues. The association decisions are most crucial near Q-fold algebraic multiplicities of eigenvalues, where eigenvectors can be arbitrarily selected as an orthogonal basis within a Q-dimensional subspace [2], thus creating challenges for an eigenvector-driven association [13].

Similar challenges exist for the analytic SVD [14]–[18], where analytic singular values can be extracted for a matrix $\boldsymbol{A}(\omega)$, $\omega \in \mathbb{R}$, over a given interval of ω, i.e. $\mathbf{A}(\omega)$ is not considered to be periodic in ω, and hence does not correspond to a discrete time function. In fact, in [15], ω is not necessarily a frequency parameter. The extraction of analytic functions in $\boldsymbol{A}(\omega)$ is driven by their arc length as a measure for smoothness [15] or by a Chebyshev interpolation. For a self-adjoint matrix $\mathbf{A}(\omega)$ (equivalent to parahermitianity on the unit circle), an analytic EVD according to Rellich exists [19], and again an algorithm for their extraction requires a suitable cost function.

Since analyticity implies infinite differentiability, in this paper we explore a suitable cost function that can distinguish between analytic and alternative (such as spectrally majorised) solutions: the power of derivatives of a function $F(\mathrm{e}^{\mathrm{j}\Omega})$. In [20], we have explored this metric and successfully applied it to drive an analytic eigenvalue extraction in [13]. The extraction algorithm in [13] aims to create associations for maximally smooth functions from an initially small but iteratively increasing number of sample points, similar to the 'missing samples problem' [21]. Any yet unassigned sample points are chosen such that a maximally smooth function for the given sample set is extracted.

In this paper, we aim to further explore the smoothness metric in [20], establish that is positive real, and introduce additional constraints onto the solution to reflect the real-valued and potentially symmetric nature of the eigenvalues of a parahermitian matrix [2]. For this, Sec. II illuminates the problem, with the interpolation of a continuous function based on samples points discussed in Sec. III. Its derivative powers are tied to the sample points in Sec. IV, followed by a

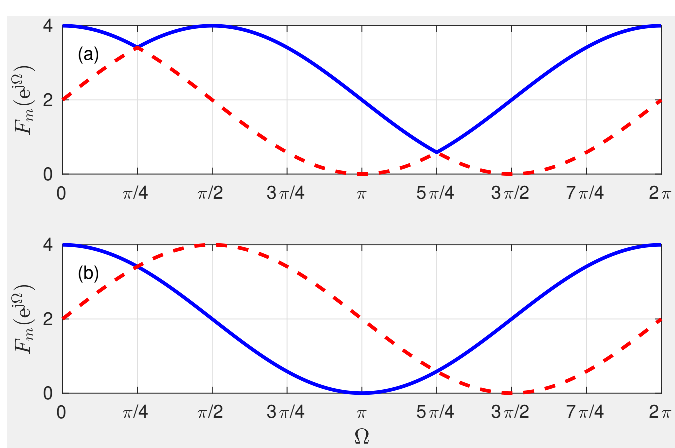

Fig. 1. (a) spectrally majorised vs (b) analytic functions.

This work was supported by the Engineering and Physical Sciences Research Council (EPSRC) Grant number EP/S000631/1 and the MOD University Defence Research Collaboration in Signal Processing.

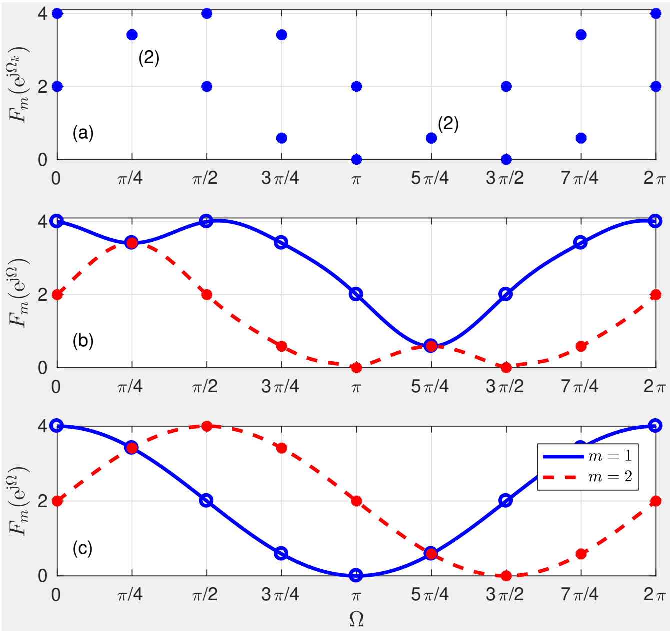

Fig. 2. (a) set of sample points for $K = 8$ and $M = 2$, and (b) spectrally majorised and (c) analytic associations of values and their interpolations.

smoothness metric for an incomplete grid of sample points is elaborated in Secs. V and VI. Finally some results and conclusions are provided in Secs. VII and VIII.

II. Problem Formulation

We are given a set of MK sample points, which is spread over K out of a total of N frequency bins and contains M values per bin. The ultimate aim is to find an association of this set to M functions that interpolate across the distinct sample points as smoothly as possible. As an example, Fig. 2 demonstrates this for a case of $N = K = 8$ and $M = 2$. The sample points are drawn in Fig. 2(a), whereby algebraic multiplicities of values greater than one are indicated in parentheses. Two different associations and their interpolation — to be discussed later — are shown in Fig. 2(b) and (c).

Thus, the challenge is to measure the smoothness of a function $F(\mathrm{e}^{\mathrm{j}\Omega})$ defined by sample points $F_k = F(\mathrm{e}^{\mathrm{j}\Omega_k})$ on a regular grid of N frequency bins $\Omega_k = 2\pi k/N$. We further specify:

(C1) only $K \le N$ sample points may be known,
(C2) $F(\mathrm{e}^{\mathrm{j}\Omega})$ is real-valued,
(C3) $F(\mathrm{e}^{\mathrm{j}\Omega})$ may be symmetric with respect to $\Omega = 0$.

As a result, we can state for its inverse Fourier transform $f[\tau]$,

$$f[\tau] = \frac{1}{2\pi}\int_{-\pi}^{\pi} F(\mathrm{e}^{\mathrm{j}\Omega})\mathrm{e}^{\mathrm{j}\Omega\tau}\mathrm{d}\Omega \; , \tag{1}$$

or in short $f[\tau] \circ\!\!-\!\!\bullet\, F(\mathrm{e}^{\mathrm{j}\Omega})$, that $f[\tau]$ must be symmetric such that $f[\tau] = f^*[-\tau]$ and that it may be real valued.

III. Dirichlet Interpolation

For $f[\tau]$ to be a symmetric sequence, it has to be of even order, or odd length. However, to align with powerful fast Fourier transform techniques, it can be advantageous to select the number of sample points N if not to be a power of two then at the very least to be even. We first address the simple case of N being odd, and thereafter focus on the more challenging case of N being even.

A. Interpolation for Odd Number of Sample Points

For N being odd, the interpolation across the sample points F_k can be accomplished by the Dirichlet kernel $P_N(\mathrm{e}^{\mathrm{j}\Omega})$,

$$P_N(\mathrm{e}^{\mathrm{j}\Omega}) = \frac{\sin\left(\frac{N}{2}\Omega\right)}{\sin\left(\frac{1}{2}\Omega\right)} = \sum_{\tau=-(N-1)/2}^{(N-1)/2} \mathrm{e}^{-\mathrm{j}\Omega\tau} \; , \tag{2}$$

which links to a rectangular window $p_N[\tau]$ that sits centred with respect to $\tau = 0$.

The kernel in (2) permits to express a 2π-periodic function $F(\mathrm{e}^{\mathrm{j}\Omega})$ as a superposition of weighted and shifted contributions,

$$F(\mathrm{e}^{\mathrm{j}\Omega}) = \frac{1}{N}\sum_{k=0}^{N-1} F_k P_N(\mathrm{e}^{\mathrm{j}(\Omega-\Omega_k)}) \tag{3}$$

$$= \frac{1}{N}\sum_{k=0}^{N-1} F_k \sum_{\tau=-(N-1)/2}^{(N-1)/2} \mathrm{e}^{-\mathrm{j}(\Omega-\Omega_k)\tau} \; , \tag{4}$$

$$= \sum_{\tau=-(N-1)/2}^{(N-1)/2} f[\tau]\mathrm{e}^{-\mathrm{j}\Omega\tau} \; , \tag{5}$$

where (4) utilises the Fourier series representation of the kernel, and $f[\tau]$ is the result of an N-point inverse discrete Fourier transform (IDFT) of $F(\mathrm{e}^{\mathrm{j}\Omega_k})$. The outcome in (5) confirms $f[\tau] \circ\!\!-\!\!\bullet\, F(\mathrm{e}^{\mathrm{j}\Omega})$, as set out in (1).

B. Interpolation for Even Number of Sample Points

The challenge for even N is exemplified in Fig. 3. When basing an inverse Fourier transform on the discrete spectrum represented by the sample points F_k of $F(\mathrm{e}^{\mathrm{j}\Omega})$, a periodised time domain $\tilde{f}[\tau] \circ\!\!-\!\!\bullet\, F(\mathrm{e}^{\mathrm{j}\Omega_k})$ emerges. For an odd number of samples points F_k, here $N = 3$, in Fig. 3(a), $f[\tau]$ can be extracted as the fundamental period of $\tilde{f}[\tau]$ in Fig. 3(b). In the even case in Fig. 3(c) and (d), $\tilde{f}[\tau]$ will be periodic with N, but also needs to be symmetric. Without loss of generality,

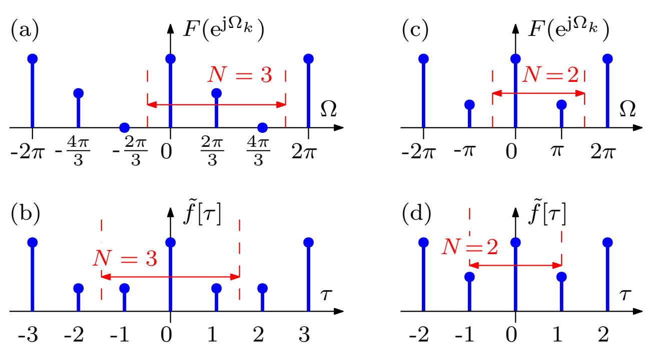

Fig. 3. Sample points for N (a) odd and (c) even, with their equivalent periodised, discrete time domain sequences in (b) and (d) respectively.

we therefore determine $\tilde{f}[\tau]$ as an inverse DFT of F_k over the interval $-N/2+1 \leq \tau \leq N/2$, and then construct $f[\tau]$ as

$$f[\tau] = \begin{cases} \tilde{f}[\tau] & |\tau| < N/2 \ , \\ \frac{1}{2}\tilde{f}[\tau] + \mathrm{j}\mathrm{sgn}\{\tau\}A & |\tau| = N/2 \ , \\ 0 & |\tau| > N/2 \ . \end{cases} \tag{6}$$

Thus, $\tilde{f}[\tau]$ emerges as a periodised version of $f[\tau]$, whereby time domain aliasing occurs at the marginal points of the interval. Note that in this periodisation, the imaginary part A is spurious, and therefore can be selected arbitrarily as $A \in \mathbb{R}$.

We define the modified Dirichlet kernel for even N as

$$P_N(\mathrm{e}^{\mathrm{j}\Omega}) = \mathrm{e}^{-\mathrm{j}\frac{\Omega}{2}} \frac{\sin\left(\frac{N}{2}\Omega\right)}{\sin\left(\frac{1}{2}\Omega\right)} = \sum_{\tau=-N/2+1}^{N/2} \mathrm{e}^{-\mathrm{j}\Omega\tau} \ .$$

Analysis similar to (3) through (5) leads to

$$F(\mathrm{e}^{\mathrm{j}\Omega}) = \sum_{\tau=-L_N}^{N-L_N-1} \tilde{f}[\tau]\mathrm{e}^{-\mathrm{j}\Omega\tau} \ , \tag{7}$$

followed by the extraction of $f[\tau]$ from (7) via (6). In (7), the summation limit uses the parameter L_N, which generalises the results for arbitrary $N \in \mathbb{N}$, whereby $L_N = N/2-1$ for N being even and $L_N = (N-1)/2$ for N being odd.

IV. Power of Derivatives of the Dirichlet Interpolation

A. Power of Derivatives

To measure the smoothness of $F(\mathrm{e}^{\mathrm{j}\Omega})$, we evaluate the power of its pth derivative,

$$\chi_p = \frac{1}{2\pi} \int_{-\pi}^{\pi} \left| \frac{\mathrm{d}^p}{\mathrm{d}\Omega^p} F(\mathrm{e}^{\mathrm{j}\Omega}) \right|^2 \mathrm{d}\Omega \ .$$

Differentiating $F(\mathrm{e}^{\mathrm{j}\Omega})$ p times with respect to the frequency parameter Ω yields

$$\begin{aligned} \frac{\mathrm{d}^p}{\mathrm{d}\Omega^p} F(\mathrm{e}^{\mathrm{j}\Omega}) &= \frac{1}{N} \sum_{k=0}^{N-1} F_k \frac{\mathrm{d}^p}{\mathrm{d}\Omega^P} P(\mathrm{e}^{\mathrm{j}(\Omega-\Omega_k)}) \\ &= \sum_{\tau=-L_N}^{N-L_N 1} (-j\tau)^p \tilde{f}[\tau] \mathrm{e}^{-\mathrm{j}\Omega\tau} \end{aligned}$$

using (7).

Note that due to orthogonality of the complex exponential terms and integration over an integer number of fundamental periods, for a Fourier series with some arbitrary coefficients b_ℓ,

$$\begin{aligned} \frac{1}{2\pi} \int_{-\pi}^{\pi} \left| \sum_l b_\ell \mathrm{e}^{\mathrm{j}\Omega\ell} \right|^2 \mathrm{d}\Omega &= \sum_\ell \frac{1}{2\pi} \int_{-\pi}^{\pi} \left| b_\ell \mathrm{e}^{\mathrm{j}\Omega\ell} \right|^2 \mathrm{d}\Omega \\ &= \sum_\ell |b_\ell|^2 \ . \end{aligned} \tag{8}$$

Therefore, given (8) we can write

$$\chi_p = \sum_{\tau=-L_N}^{N-L_N-1} \left| (-\mathrm{j}\tau)^p \tilde{f}[\tau] \right|^2 = \sum_{\tau=-L_N}^{N-L_N-1} \tau^{2p} |\tilde{f}[\tau]|^2 \ ,$$

i.e. the power of the derivatives can be entirely calculated based on the time domain samples $\tilde{f}[\tau]$.

B. Matrix Formulation

An N-point DFT matrix $\mathbf{T}_N$ is normalised such that $\mathbf{T}_N \mathbf{T}_N^{\mathrm{H}} = \mathbf{I}$. Based on the permutation matrix $\mathbf{P} \in \mathbb{N}^{N\times N}$ to exert a DFT shift,

$$\mathbf{P} = \left[\begin{array}{c|c} \mathbf{0}_{L_N \times N-L_N} & \mathbf{I}_{L_N} \\ \hline \mathbf{I}_{N-L_N} & \mathbf{0}_{N-L_N \times L_N} \end{array} \right] \ , \tag{9}$$

the coefficient vectors $\underline{F} \in \mathbb{R}^N$ and $\tilde{\mathbf{f}} \in \mathbb{C}^N$,

$$\begin{aligned} \underline{F} &= [F_0, \ F_1, \ \ldots, \ F_{N-1}]^{\mathrm{T}} \\ \tilde{\mathbf{f}} &= \left[\tilde{f}[-L_N], \ \ldots, \ \tilde{f}[N-L_N-1] \right]^{\mathrm{T}} \ , \end{aligned} \tag{10}$$

relate as $\tilde{\mathbf{f}} = \frac{1}{\sqrt{N}} \mathbf{P}\mathbf{T}_N^{\mathrm{H}} \underline{F}$. The organisation of $\tilde{\mathbf{f}}$ in (10), being centred with respect to $\tau = 0$ according to Fig. 3(b) and (d), requires the DFT shift by $\mathbf{P}$ in (9).

Further, we define

$$\mathbf{D} = \mathrm{diag}\{(-L_N), \ \ldots, \ 0, \ldots, \ (N-L_N-1)\} \ ,$$

such that

$$\chi_p = \tilde{\mathbf{f}}^{\mathrm{H}} \mathbf{D}^{2p} \tilde{\mathbf{f}} = \frac{1}{N} \underline{F}^{\mathrm{H}} \mathbf{T}_N \mathbf{P}^{\mathrm{H}} \mathbf{D}^{2p} \mathbf{P} \mathbf{T}_N^{\mathrm{H}} \underline{F} \ .$$

If power is accumulated across several derivatives up to order P, $\chi^{(P)} = \sum_{p=0}^{P} \chi_p$, then with the abbreviation

$$\mathbf{C} = \frac{1}{N} \mathbf{T}_N \mathbf{P}^{\mathrm{H}} \sum_{p=0}^{P} \mathbf{D}^{2p} \mathbf{P} \mathbf{T}_N^{\mathrm{H}} \ ,$$

we can evaluate the cost as a weighted inner product $\chi^{(P)} = \underline{F}^{\mathrm{H}} \mathbf{C} \underline{F}$. Since the inner part $\mathbf{P}^{\mathrm{H}} \sum_{p=0}^{P} \mathbf{D}^{2p} \mathbf{P}$ is real valued and diagonal, with a symmetric sequence occupying this diagonal, $\mathbf{C}$ necessarily is a circulant matrix comprising of real-valued entries [22].

V. Constrained Optimisation

Algorithms for the extraction of analytic eigenvalues often require to measure the smoothness of function segments based on a limited number of sample point [13]. This, together with additional conditions on $F(\mathrm{e}^{\mathrm{j}\Omega})$, is in this section addressed as an optimisation problem on the time domain coefficients in a stacked vector $\boldsymbol{f}^{\mathrm{T}} = [\tilde{\mathbf{f}}_{\mathrm{r}}^{\mathrm{T}} \ \tilde{\mathbf{f}}_{\mathrm{i}}^{\mathrm{T}}]$,

$$\min_{\boldsymbol{f}} \boldsymbol{f}^{\mathrm{H}} \boldsymbol{\Delta} \boldsymbol{f} \qquad \text{such that} \quad \mathbf{G}\boldsymbol{f} = \mathbf{b} \ , \tag{11}$$

with appropriate quantities $\boldsymbol{\Delta}$, $\mathbf{G}$ and $\mathbf{b}$ to be defined below. We embed up to three different conditions on $F(\mathrm{e}^{\mathrm{j}\Omega})$:

C1: If only a limited number of sample points $K \leq N$ are available, then we define a selection matrix $\mathbf{S} \in \mathbb{Z}^{K\times N}$ that relates this reduced set $\underline{F}^{(r)}$ to $\underline{F}$ and $\tilde{\mathbf{f}}$ as

$$\underline{F}^{(r)} = \mathbf{S}\underline{F} = \sqrt{N} \mathbf{S} \mathbf{T}_N \mathbf{P}^{\mathrm{H}} \tilde{\mathbf{f}} = \mathbf{A}\tilde{\mathbf{f}} \ ,$$

or

$$\begin{bmatrix} \mathrm{Re}\{\mathbf{A}\} & -\mathrm{Im}\{\mathbf{A}\} \\ \mathrm{Im}\{\mathbf{A}\} & \mathrm{Re}\{\mathbf{A}\} \end{bmatrix} \boldsymbol{f} = \begin{bmatrix} \underline{F}^{(r)} \\ \underline{0}_K \end{bmatrix} . \quad (12)$$

C2: $F(\mathrm{e}^{\mathrm{j}\Omega})$ is real-valued $\leftrightarrow$ $f[\tau]$ is symmetric, i.e. $f[\tau] = f^*[-\tau]$, which imposes the constraint

$$\begin{bmatrix} \mathbf{I}_{L_N} & -\mathbf{K}_N & \mathbf{0}_{L_N \times N} \\ \mathbf{0}_{L_N \times N} & \mathbf{I}_{L_N} & \mathbf{K}_N \end{bmatrix} \boldsymbol{f} = \underline{0} , \quad (13)$$

with $\mathbf{K}_N$ given via the $L_n \times L_n$ reverse identity $\mathbf{J}_{L_N}$

$$\mathbf{K}_N = \begin{cases} [\underline{0}\ \mathbf{J}_{L_N}\ \underline{0}] & N \text{ even} \\ [\underline{0}\ \mathbf{J}_{L_N}] & N \text{ odd} . \end{cases}$$

C3: For a symmetric $F(\mathrm{e}^{\mathrm{j}\Omega})$, we can demand $f[\tau]$, and therefore also $\tilde{f}[\tau]$, to be real-valued:

$$\tilde{\mathbf{f}}_{\mathrm{i}} = \underline{0}_N .$$

Thus, for constraints C1 and C2, the overall constraint in (11) will be drawn from (13) and (12), such that $\mathbf{G} \in \mathbb{R}^{2(L_N+K)\times 2N}$ and $\mathbf{b} \in \mathbb{R}^{2(L_N+K)}$. For $K > N - L_N$, the constraint equation will be an overdetermined system, and it will either be possible to condense the constraint equation $\mathbf{G}\boldsymbol{f} = \mathbf{b}$ via an SVD similar to robust MVDR beamforming [23], or in case it is approximately full rank, entirely via $\boldsymbol{f} = \mathbf{G}^{\dagger}\mathbf{b}$, with $\{\cdot\}^{\dagger}$ denoting the pseudo-inverse. Otherwise, with $\boldsymbol{\Delta} = \sum_{p=0}^{P} \mathrm{blockdiag}\{\mathbf{D}^{2p},\ \mathbf{D}^{2p}\}$, the solution to the optimisation problem is analogous to the Capon or minimum variance distortionless response beamformer, with [20]

$$\chi_{\min} = \mathbf{b}^{\mathrm{H}}(\mathbf{G}\boldsymbol{\Delta}^{-1}\mathbf{G}^{\mathrm{H}})^{\dagger}\mathbf{b} .$$

Constraint C3 can be combined with C1 and C2 by purging any reference to $\tilde{\mathbf{f}}_{\mathrm{i}}$, and therefore condensing the constraints such that

$$\mathbf{G} = \begin{bmatrix} \mathrm{Re}\{\mathbf{A}\} \\ \mathbf{I}_{L_N} \quad -\mathbf{K}_N \end{bmatrix} , \qquad \mathbf{b} = \begin{bmatrix} \underline{F}^{(r)} \\ \underline{0}_{L_N} \end{bmatrix} ,$$

followed by optimisation for $\boldsymbol{f} = \tilde{\mathbf{f}}_{\mathrm{r}}$ only.

VI. Schur Complement

An alternative approach to Sec. V is to solve $\chi^{(P)} = \underline{F}^{\mathrm{H}}\mathbf{C}\underline{F}$ under the conditions C1–C3 via the Schur complement of $\mathbf{C}$ directly for the sample points in $\underline{F}$. For this, we define $\underline{F}^{(\mathrm{q})}$ as containing $\underline{F}^{(\mathrm{r})}$ as well as any additional components due to the symmetry condition C3, such that

$$\begin{bmatrix} \underline{F}^{(\mathrm{q})} \\ \mathbf{x} \end{bmatrix} = \begin{bmatrix} \mathbf{S}_{\mathrm{q}} \\ \mathbf{S}_{\mathrm{q}}^{\perp} \end{bmatrix} \underline{F} = \boldsymbol{\Sigma}\underline{F}$$

with $\mathbf{S}_{\mathrm{q}} \in \mathbb{Z}^{L\times N}$ a binary selection matrix similar to $\mathbf{S} \in \mathbb{Z}^{K\times N}$ but potentially with added rows to reflect the symmetry condition C3, i.e. $K \leq L < 2K$, and $\mathbf{S}_{\mathrm{q}}^{\perp}$ its orthogonal complement.

The matrix $\mathbf{B} = \boldsymbol{\Sigma}\mathbf{C}\boldsymbol{\Sigma}^{\mathrm{T}} \in \mathbb{R}^{N\times N}$ can be partitioned as

$$\mathbf{B} = \begin{bmatrix} \mathbf{B}_1 & \mathbf{B}_2 \\ \mathbf{B}_2^{\mathrm{T}} & \mathbf{B}_4 \end{bmatrix} ,$$

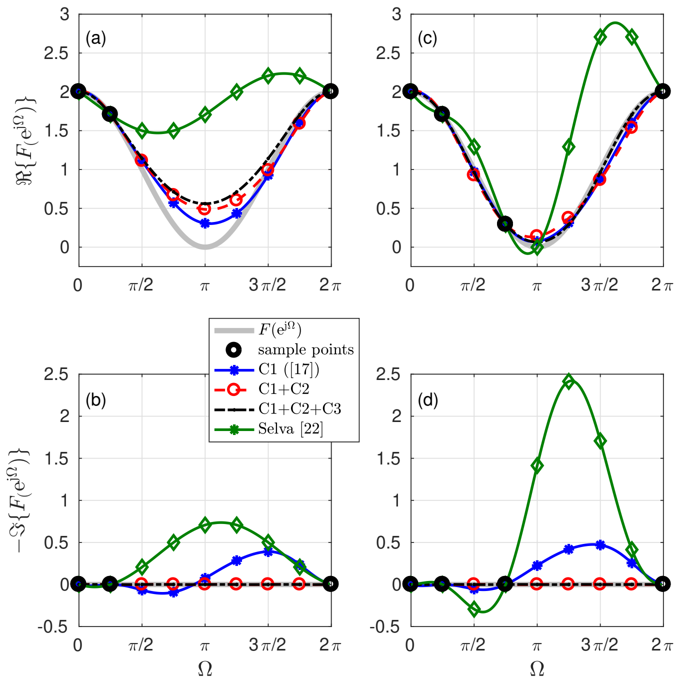

Fig. 4. Smooth approximations of $F(\mathrm{e}^{\mathrm{j}\Omega})$ using various interpolation approaches given (a,b) $K = 2$ and (c,d) $K = 3$ sample points.

with $\mathbf{B}_1 \in \mathbb{R}^{L\times L}$ and all other components of appropriate dimensions. Based on the solution to $\min_{\mathbf{x}} [\underline{F}^{(\mathrm{q}),\mathrm{T}}\ \ \mathbf{x}^{\mathrm{T}}]\mathbf{B}[\underline{F}^{(\mathrm{q}),\mathrm{T}}\ \ \mathbf{x}^{\mathrm{T}}]^{\mathrm{T}}$, the smoothness metric for the optimal completion $\mathbf{x}$ is given by [20]

$$\chi_{\min} = \underline{F}^{(\mathrm{q}),\mathrm{T}}(\mathbf{B}_1 - \mathbf{B}_2\mathbf{B}_4^{-1}\mathbf{B}_2^{\mathrm{T}})\underline{F}^{(\mathrm{q})}$$

via the Schur complement $\mathbf{B}_1 - \mathbf{B}_2\mathbf{B}_4^{-1}\mathbf{B}_2^{\mathrm{T}}$ of $\mathbf{B}$, but which differently from [20] incorporates the additional constraints.

VII. Results and Discussion

We first provide an example for the interpolations achieved by various settings, benchmarked against [20] and [21], whereby the latter aims to achieve a time domain response that does not exceed a support of K, without explicit desire for smoothness but at minimal computational cost. In Fig. 4, we see a sampling grid of $N = 8$ for the function $F(\mathrm{e}^{\mathrm{j}\Omega}) = 1 + \cos\Omega$, and are given (i) $K = 2$ sample points for $k = \{0, 1\}$ and (ii) $K = 3$ sample points for $k = \{0, 1, 3\}$. As the number of sample points increases, the interpolated function is further tied down and therefore better approximates the original $F(\mathrm{e}^{\mathrm{j}\Omega})$. A similar effect can be observed as more constraints are taken on board. Constraining the missing sample points to be real valued provides a small enhancement and eliminates any deviation in the imaginary part, while the symmetry condition essentially increases the number of given sample points.

When checking on the Pth derivative power σ_P^2 of an interpolation based on K given sample points of the above $F(\mathrm{e}^{\mathrm{j}\Omega})$, the metrics in Tab. I for $P = 5$ are returned. Note that as K and the number of constraints increases, the values converge towards the true $\sigma_P^2 = \frac{1}{2}$. The approach by

TABLE I

POWER IN THE $P = 4$TH DERIVATIVE OF AN INTERPOLATION DRIVEN BY A COST FUNCTION WITH $P = 4$ FOR A VARIABLE NUMBER K OF SAMPLE POINTS ON A GRID $N = 8$.

K	C1 [20]	C1+C2	C1+C2+C3	Selva [21]
2	0.152832	0.196791	0.401503	0.146447
3	0.438293	0.445379	0.488754	5.707107
4	0.493379	0.493481	0.499909	51.935029
5	0.499571	0.499572	0.500000	297.524387
6	0.499368	0.499368	0.500000	761.419354
7	0.499929	0.499929	0.500000	333.250000
8	0.500000	0.500000	0.500000	0.500000

Selva [21], which aims to solve the missing samples problem by providing an interpolation for a compact $f[\tau] \circ\!\!-\!\!\bullet\, F(e^{j\Omega})$ via a highly efficient fast Fourier transform scheme, does not offer the smooth interpolation that we seek.

Without the additional constraints C1–C3, in [20] the constraint optimisation was found to have lower complexity and better conditioning compared to the Schur approach for $K \ll N$, and vice versa for $K \rightarrow N$. Here, with additional constraints, the cost is shifted: MVDR is computationally more expensive due to the increased dimension of the constraint matrix, while the Schur complement scheme — dominated the matrix inverse of $\mathbf{B}_4$ — contents with a lower dimension and therefore lower cost.

VIII. CONCLUSIONS

This paper has illuminated properties of a cost function that evaluates the power of derivatives from the smoothest possible interpolation through a potentially incomplete number of sample points on the unit circle. The particular type of function to be interpolated here are eigenvalues, which in the Fourier domain will be non-negative, real-valued, and can potentially be symmetric. The cost function can be evaluated as a weighted inner product of the coefficient vector, whereby the weighting matrix is real-valued and circulant.

The real-valuedness and potential symmetry of eigenvalues can be enforced by constraints, which also aids in matching the power of the derivatives of an approximated function more closely. We have benchmarked this method against the previously existing approach in [20], and compared it to a low-cost interpolation in [21]. The latter is not aimed at providing a maximally smooth interpolation but sets an aspiration in terms of its very low computational footprint.

Therefore, the proposed metric offers some good properties for the extraction of analytic factors for, for example, the EVD of an analytic, parahermitian matrix [12], [13]. Analyticity in turn offers the opportunity of Laurent polynomial approximations that can be siginificantly lower in order than for factors that are obtained by current time domain algorithms favouring spectral majorisation [4], [5], [7], [9]. With lower order polynomials translating into lower implementation cost, the proposed metric may directly contribute to reduced computational cost for applications such as broadband beamforming [24], angle or arrival estimation [25], or source separation [26].

REFERENCES

[1] P. P. Vaidyanathan, *Multirate Systems and Filter Banks*, Prentice Hall, Englewood Cliffs, 1993.

[2] S. Weiss, J. Pestana, and I.K. Proudler, "On the existence and uniqueness of the eigenvalue decomposition of a parahermitian matrix," *IEEE TSP*, **66**(10):2659–2672, May 2018.

[3] S. Weiss, J. Pestana, I.K. Proudler, and F.K. Coutts, "Corrections to 'On the existence and uniqueness of the eigenvalue decomposition of a parahermitian matrix'," *IEEE TSP*, **66**(23):6325–6327, Dec. 2018.

[4] J.G. McWhirter, P.D. Baxter, T. Cooper, S. Redif, and J. Foster, "An EVD Algorithm for Para-Hermitian Polynomial Matrices," *IEEE Trans. SP*, **55**(5):2158–2169, May 2007.

[5] S. Redif, J.G. McWhirter, and S. Weiss, "Design of FIR paraunitary filter banks for subband coding using a polynomial eigenvalue decomposition," *IEEE Trans. SP*, **59**(11):5253–5264, Nov. 2011.

[6] J. Corr, K. Thompson, S. Weiss, J.G. McWhirter, S. Redif, and I.K. Proudler, "Multiple shift maximum element sequential matrix diagonalisation for parahermitian matrices," in *IEEE SSP*, Gold Coast, Australia, June 2014, pp. 312–315.

[7] S. Redif, S. Weiss, and J.G. McWhirter, "Sequential matrix diagonalization algorithms for polynomial EVD of parahermitian matrices," *IEEE Trans. SP*, **63**(1):81–89, Jan. 2015.

[8] Z. Wang, J. G. McWhirter, J. Corr, and S. Weiss, "Multiple shift second order sequential best rotation algorithm for polynomial matrix EVD," in *EUSIPCO*, Nice, France, Sep. 2015, pp. 844–848.

[9] J.G. McWhirter and Z. Wang, "A novel insight to the SBR2 algorithm for diagonalising para-hermitian matrices," in *IMA Maths in Signal Proc.*, Birmingham, UK, Dec. 2016.

[10] M. Tohidian, H. Amindavar, and A.M. Reza, "A DFT-based approximate eigenvalue and singular value decomposition of polynomial matrices," *J. Adv. SP*, **2013**(1):1–16, 2013.

[11] F.K. Coutts, K. Thompson, S. Weiss, and I.K. Proudler, "A comparison of iterative and DFT-based polynomial matrix eigenvalue decompositions," in *IEEE CAMSAP*, Curacao, Dec. 2017.

[12] F.K. Coutts, K. Thompson, J. Pestana, I.K. Proudler, S. Weiss, "Enforcing eigenvector smoothness for a compact DFT-based polynomial eigenvalue decomposition," in *IEEE SAM*, Sheffield, UK, July 2018.

[13] S. Weiss, I.K. Proudler, F.K. Coutts, and J. Pestana, "Iterative approximation of analytic eigenvalues of a parahermitian matrix EVD," in *IEEE ICASSP*, Brighton, UK, May 2019.

[14] B.L.R. De Moor and S.P. Boyd, "Analytic properties of singular values and vectors," Tech. Rep., KU Leuven, 1989.

[15] A. Bunse-Gerstner, R. Byers, V. Mehrmann, and N.K. Nicols, "Numerical computation of an analytic singular value decomposition of a matrix valued function," *Numer. Math.*, **60**:1–40, 1991.

[16] K. Wright, "Differential equations for the analytic singular value decomposition of a matrix," *Numer. Math.*, **63**(1):283–295, Dec. 1992.

[17] L. Dieci and T. Eirola, "On smooth decompositions of matrices," *SIAM J. Matrix Analysis and Applications*, **20**(3):800–819, 1999.

[18] E.S. Van Vleck, *Numerical algebra, matrix theory, differential-algebraic equations and control theory*, chapter Continuous Matrix Factorizations, pp. 299–318, Springer, 2015.

[19] F. Rellich, "Störungstheorie der Spektralzerlegung. I. Mitteilung. Analytische Störung der isolierten Punkteigenwerte eines beschränkten Operators," *Math. Annalen*, **113**:DC–DCXIX, 1937.

[20] S. Weiss and M.D. Macleod, "Maximally smooth Dirichlet interpolation from complete and incomplete sample points on the unit circle," in *IEEE ICASSP*, Brighton, UK, May 2019.

[21] J. Selva, "FFT interpolation from nonuniform samples lying in a regular grid," *IEEE TSP*, **63**(11):2826–2834, June 2015.

[22] G.H. Golub and C.F. Van Loan, *Matrix Computations*, John Hopkins University Press, Baltimore, Maryland, 3rd edition, 1996.

[23] R.G. Lorenz and S.P. Boyd, "Robust minimum variance beamforming," *IEEE TSP*, **53**(5):1684–1696, May 2005.

[24] S. Weiss, S. Bendoukha, A. Alzin, F.K. Coutts, I.K. Proudler, and J.A. Chambers, "MVDR broadband beamforming using polynomial matrix techniques," in *EUSIPCO*, Nice, Sep. 2015, pp. 839–843.

[25] M. Alrmah, S. Weiss, and S. Lambotharan, "An extension of the MUSIC algorithm to broadband scenarios using polynomial eigenvalue decomposition," in *EUSIPCO*, Barcelona, Aug. 2011, pp. 629–633.

[26] S. Redif, S. Weiss, and J.G. McWhirter, "Relevance of polynomial matrix decompositions to broadband blind signal separation," *Sig. Proc.*, **134**:76–86, May 2017.